Turk J Elec Engin, VOL.14, NO.3 2006, © TÜBİTAK

The Effect of Collector Doping on InP-Based Double Heterojunction Bipolar Transistors

Serkan TOPALOĞLU, Jörn DRIESEN, Werner PROST, Franz Josef TEGUDE
Solid State Electronics Department, Faculty of Engineering
University Duisburg - Essen, 47057, Duisburg-GERMANY
e-mail: topaloglu@hlt.uni-duisburg.de - serkant@ieee.org

Abstract

High current effects on double heterojunction bipolar transistor (DHBT) performance were investigated. Three DHBTs with different collector doping densities were grown and processed. DC and RF measurements were performed to evaluate the influence of collector doping and the related Kirk effect on HBT performance. In addition to these samples, the Kirk effect was proven on SHBTs and the delay of this effect on submicron HBTs was investigated.

1. Introduction

Due to advances in optical communication systems, InP-based heterojunction bipolar transistors (HBTs) have been intensively investigated in recent years. One of the main advantages of this material is its compatibility with optoelectronic devices operating at the 1.3 and 1.55 μm communication wavelengths, where optical attenuation is at its minimum. Moreover, since HBTs have high transconductance, high current density, and excellent RF behaviour, they are also attractive for high-speed electronic applications.

The figures of merit for high frequency performance are the cut-off frequency, f_T, and the maximum frequency of oscillation, f_{max} [1].

$$\frac{1}{2\pi \cdot f_T} = \tau_{base} + \tau_{collector} + C_{je}\frac{kT}{qI_E} + C_{jc}\left(\frac{kT}{qI_E} + R_{ex} + R_{coll}\right) \quad (1)$$

$$f_{\max} \cong \sqrt{\frac{f_T}{8\pi \cdot R_{bb}C_{bc}}} \quad (2)$$

As depicted in Eq. 1, the cut-off frequency is limited by the transition times, which are mostly influenced by the vertical design of the HBT structure. In contrast to this, the maximum oscillation frequency is mostly affected by the parasitic capacitances and resistances, which can be controlled by lateral scaling of the devices. Briefly, f_T can be improved by epitaxy and the processing and layout can improve f_{max}.

To achieve higher f_{max}, several techniques have been introduced in the literature. These are base undercut, transferred substrate HBTs, and buried collector HBTs, in which the parasitic base-collector (C_{bc}) can be reduced [2-8].

By decreasing the base and collector thickness, the transit frequency, f_T, can be improved, but at the same time, f_{max} may be adversely affected.

In this work, we investigated the effect of collector doping on HBT's RF performance. When the collector current increases ($J_C > qN_{dC}v_{sat}$), the electron density entering the base-collector depletion region exceeds the doping level and this changes the electric field profile in the junction. This will cause an increase in hole injection from the base to collector and, therefore, an increase in the base width. Since there is a greater distance for carriers to penetrate, this will degrade the current gain and increase the base transit time. Doping the collector can minimise this situation. Details about the Kirk effect have been explained in [9, 10].

2. Experiment

The epitaxial layer structure used for fabrication of the devices is listed in Table 1.

Table 1. The layer structure of the processed DHBTs.

n++ InGaAs	E-Cap	50 nm
n+ InP	E-contact	50 nm
n InP	Emitter	50 nm
p InGaAs	Base	50 nm
InGaAs	Spacer	30 nm
InGaAsP	Quaternary layer	10 nm
InGaAsP	Quaternary layer	20 nm
InP	Collector	100 nm
n+ InP	Collector contact	100 nm
n++ InGaAs	Sub-collector	200 nm
InP	Buffer	50 nm
s.i. InP Substrate		

The structure is grown by LP-MOVPE (low-pressure metal-organic vapour-phase epitaxy) (Aixtron 200) on (001) $\pm$ 0.5° -oriented semi insulating (001) InP (Fe) substrate [11]. Three samples are used for this investigation. Samples A, B, and C have the same layer structure depicted in Table 1, but the collector doping densities differ. The collector doping densities are non-intentionally doped (NID), $5 \times 10^{16} cm^{-3}$, and $5 \times 10^{17} cm^{-3}$ for samples A, B, and C, respectively. These samples are processed in parallel to eliminate any deviation that may occur due to environmental effects during processing.

The device fabrication is carried out by conventional wet chemical etching, based on phosphoric acid (H_3PO_4) for InGaAs and InGaAsP layers, and hydrochloric acid (HCl) for InP layers. The emitter, base, and collector layers are defined by optical lithography. The Ti/Pt/Au contact metal system is used for emitter and collector contacts. The self-aligned base contact metallisation is deposited as Pt/Ti/Pt/Au. Traditionally, air bridges are used for the connections to the measurement pads. A scanning electron microscope (SEM) photograph of one of the realised HBTs is shown in Figure 1.

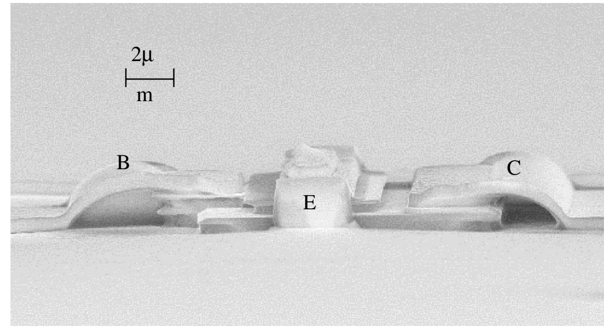

Figure 1. SEM photograph of an HBT with nominal $A_E = 2 \times 10\ \mu m^2$.

3. Results and Discussion

The DC characteristics of the DHBTs were measured by an HP4515B parameter analyser.

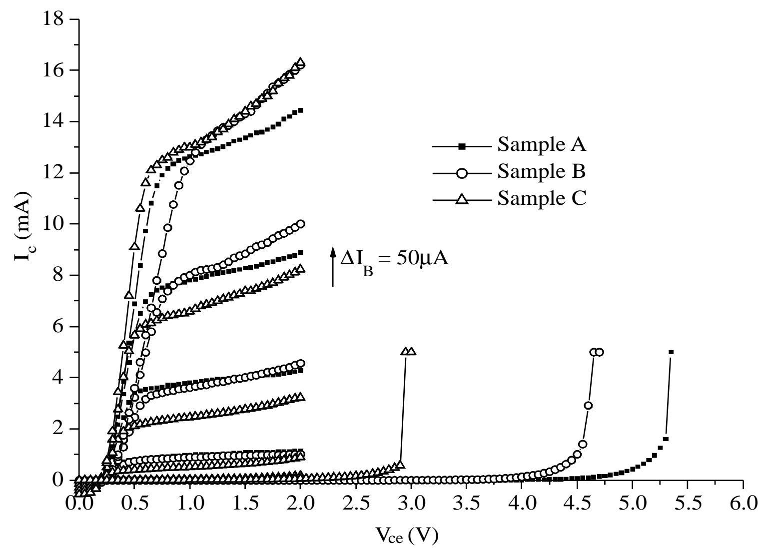

Figure 2. The common emitter output characteristics for samples A, B, and C (nominal $A_E = 2 \times 10\ \mu m^2$).

In Figure 2, the common emitter output characteristic for samples A, B, and C are shown. The DC current gain is nearly 70 for these 3 samples at $I_B = 200\ \mu A$.

In Figures 3, 4, and 5, the high current regions are marked with a dashed circle. In these circles, the Kirk effect can be identified by the sudden increase in the base current (I_B) and a slight decrease in the collector current (I_C).

From these Gummel plots, it can be concluded that, due to the increased doping density of the collector, the current density (J_{Kirk}) where the high current effects appear has also increased [12].

On the other hand, the breakdown voltage has decreased by increasing collector doping density ($BV_{CE,sampleA} = 5.5$ V, $BV_{CE,\ sampleB} = 4.5$ V, $BV_{CE,sampleC} = 3$ V).

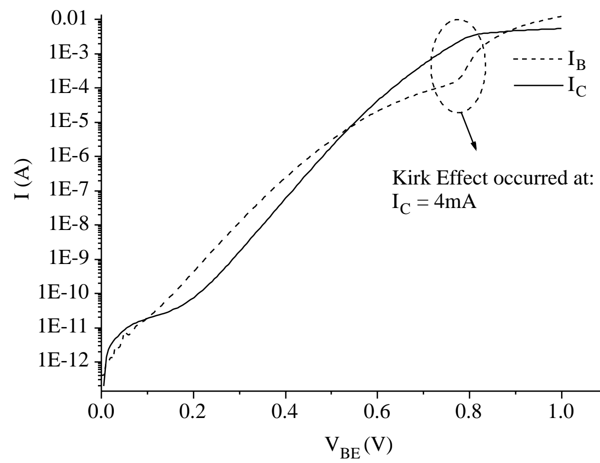

Figure 3. The Gummel plot for sample A.

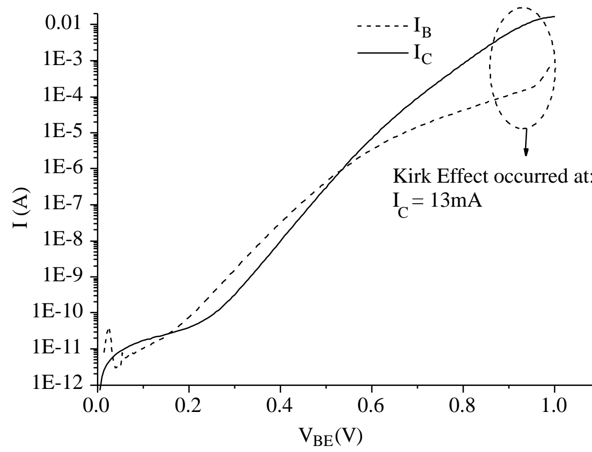

Figure 4. The Gummel plot for sample B.

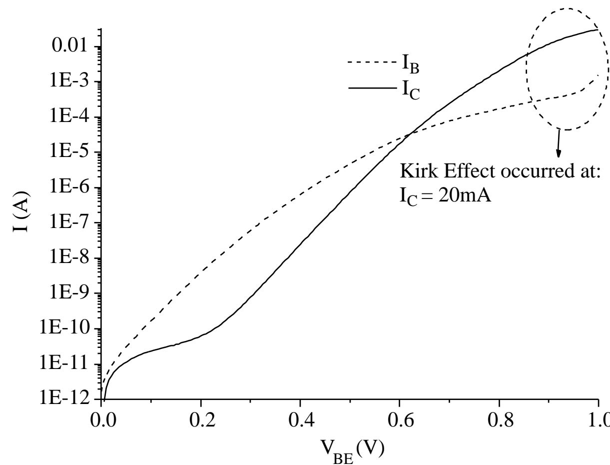

Figure 5. The Gummel plot for sample C.

After achieving these results from the DC measurements, RF measurements were performed using an HP8510C network analyser. For these measurements, again, the same devices ($A_E = 2 \times 10\ \mu m^2$) was

used. Here, samples A, B, and C have shown a cut-off frequency (f_T) of 100, 120, and 165 GHz, respectively.

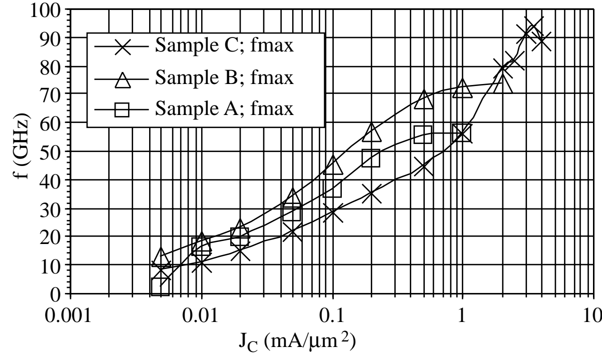

Figure 6. The maximum oscillation frequency of DHBTs vs. current density.

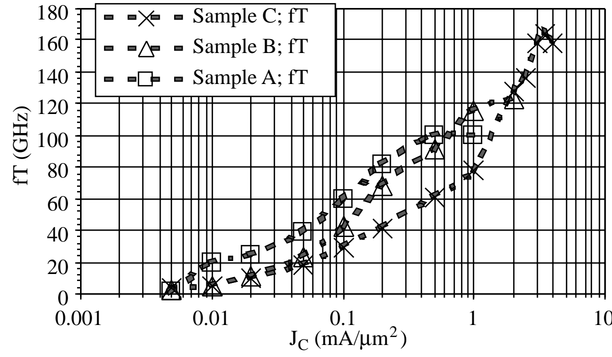

Figure 7. The cut-off frequency of DHBTs vs. current density.

These results are also confirmed with calculations using Eqs. 3 and 4 [10].

$$J_{Kirk} = (1 + \frac{V_{CB} + \phi_{CB}}{V_2 + \phi_{CB}})\, q\, N_C\, v_{sat} \tag{3}$$

$$\phi_{CB} = \frac{E_g}{2} + \frac{kT}{q}\ln(\frac{N_C}{n_i}) \tag{4}$$

where

ϕ_{CB} Base-collector junction potential
V_2 applied base-collector bias that totally depletes collector layer when $J_C = 0$
N_C Collector doping density
v_{sat} Saturation velocity

The calculated Kirk current densities (J_{Kirk}) are $J_{Kirk,A} = 0.8$ mA/μm^2, $J_{Kirk,B} = 2$ mA/μm^2, and $J_{Kirk,C} = 4$ mA/μm^2. As it can be extracted from Figure 6, the maximum current densities are $J_{Cmax,A} = 0.5$ mA/μm^2, $J_{Cmax,B} = 1.5$ mA/μm^2, and $J_{Cmax,C} = 3.5$ mA/μm^2. Here, the maximum current density is mostly influenced by the Kirk effect and these values fit fairly well with the calculations.

In addition to DHBTs, the same phenomena were examined for SHBTs. For this purpose, 2 SHBTs with NID and 5×10^{17}cm^{-3} collector doping densities were grown and processed. These samples are

referred to as samples X and Y, respectively. The layer structures for these SHBTs are presented in Table 2. These samples have been processed in the same manner as explained for DHBTs.

Table 2. The layer structure of the processed SHBTs.

n++ InGaAs	E-Cap	50 nm
n+ InP	E-contact	50 nm
n InP	Emitter	50 nm
p InGaAs	Base	50 nm
InGaAs	Collector	600 nm
InP	Stop etch	10 nm
n++ InGaAs	Sub-collector	300 nm
InP	Buffer	50 nm
s.i. InP Substrate		

The RF measurements showed that sample X has the Kirk current density of 0.3 mA/μm^2, whereas sample Y's is 1 mA/μm^2. The calculated Kirk current densities are 0.4 mA/μm^2 and 1.2 mA/μm^2 for samples X and Y, respectively. Cut-off frequencies of 90 and 170 GHz were measured for samples X and Y, respectively. Sample Y has a 330 GHz maximum oscillation frequency. The significant improvement in the maximum oscillation frequency for SHBTs compared to DHBTs is due to the missing quaternary layer and thicker collector layer, which offer higher collector undercut and reduce the parasitic base-collector capacitances.

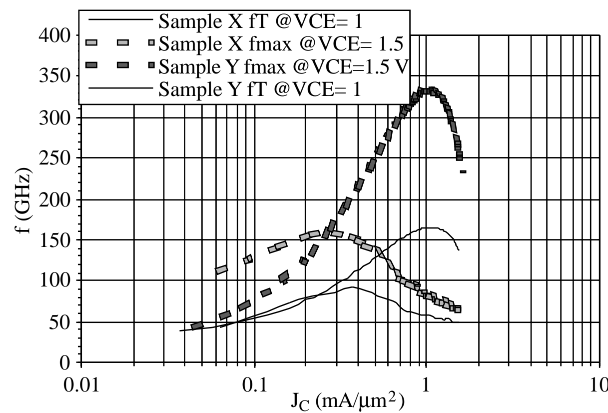

Figure 8. The RF performance of SHBTs vs. the current density for 1 × 15 μm^2 devices.

Moreover, on sample Y, the sub-micron emitters are realised by using ICP-RIE etching [13]. An SEM photograph of the processed 0.5 × 7.5 mA/μm^{2}SHBT is shown in Figure 9.

The RF measurements were performed for this device and it was observed that the Kirk current density is nearly 3 mA/μm^2, which was nearly 1.2 mA/μm^2 for the 1 × 15 μm^2 device. The improvement in the current density is attributed to the collector current spreading effect. At high injection levels, the carriers diffuse outwards when they enter the collector because of the lateral concentration gradient that exists in the depletion region. The amount of spreading can be approximated as:

$$L_D = \sqrt{D.\tau} \tag{5}$$

where L_D is the amount of spreading, D is the high field diffusion constant, and τ is the collector transit time. The transit time is determined by the collector thickness (t_C) and the average drift velocity, υ_s. This means that L_D is mostly determined by the layer structure and is independent of the lateral design of HBTs. For our SHBTs, L_D was estimated to be 0.4 μm. This value becomes much more important when the emitter width gets smaller. The shift in the Kirk current density can be explained in this manner [14].

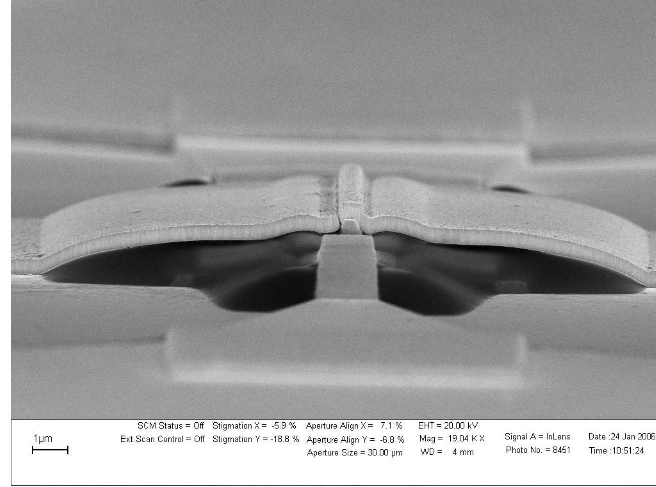

Figure 9. SEM photograph of a sub-micron HBT with nominal $A_E = 0.5 \times 7.5\ \mu m^2$.

4. Conclusion

The Kirk effect was experimentally observed by DHBT performance. To analyse the effect, DC measurements were performed. With the help of Gummel plots, the point where the Kirk effect occurs, J_{Kirk} (the point where a sudden increase in base current occurs), was identified. It has been concluded that doping the collector can reduce this effect. This will lead to better RF performance; but a compromise is necessary, because, when the collector is doped, the breakdown voltage decreases, as shown in Table 3.

Table 3. The layer structure of the processed DHBTs.

Sample	Collector Doping Density (N_c) (cm^{-3})	$J_{Cmax,measured}$ ($mA/\mu m^2$)	$J_{Kirk,calculated}$ ($mA/\mu m^2$)	f_T (GHz)	f_{max} (GHz)	BV_{CEO} (V)
Sample A	NID	0.5	0.8	100	60	5.5
Sample B	5×10^{16}	1.5	2	120	75	4.5
Sample C	5×10^{17}	3.5	4	165	95	3.0

All these experimental results were compared with the theoretical calculations and good fits have been achieved. In addition to the DHBTs, the same effect was investigated for SHBTs and similar behaviour has been observed. On the other hand, sub-micron HBTs have been realised and it was proven that the Kirk current density can be improved for smaller structures due to the delay of the Kirk effect.

References

[1] M. Rodwell, et al., "Submicron scaling of HBTs Electron Devices," *IEEE Transactions on Electron Devices*, Volume 48, Issue 11, pp. 2606-2624, Nov. 2001.

[2] S. Lee, et al., "Ultra high f_{max} InP/InGaAs/InP transferred substrate DHBTs," *60th DRC Conference Digest* 24-26 pp. 107-108, June 2002.

[3] Q. Lee, et al., "A>400 GHz f_{max} transferred-substrate heterojunction bipolar transistor IC technology," *Electron Device Letters, IEEE* Volume 19, Issue 3, pp. 77-79, March 1998.

[4] S. Lee, et al., "Transferred-substrate InP/InGaAs/InP double heterojunction bipolar transistors with f_{max} = 425 GHz," *Electronics Letters*, Volume 37, Issue 17, 16, pp. 1096 – 1098, Aug. 2001.

[5] H. Sato, et al., "InGaAs/InAlAs/InP collector-up microwave heterojunction bipolar transistors," *Electron Device Letters, IEEE,* Volume 11, Issue 10, pp. 457-459, Oct. 1990.

[6] L. Kyungho, et al., "New Collector Undercut Technique Using a SiN Sidewall for Low Base Contact Resistance in InP/InGaAs SHBTs," *IEEE Transactions on Electron Devices,* Vol. 49, No. 6, pp. 1079-1082, June 2002.

[7] T. Arai, et al., "C_{BC} reduction in GaInAs/InP buried metal heterojunction bipolar transistor," *Indium Phosphide and Related Materials*, 14-18, pp. 254-257, May 2000.

[8] S. Topaloglu, J. Driesen, A. Poloczek, F. -J Tegude, 'Fabrication of Transferred-Substrate HBT with Simple Technology', *The17th Indium Phosphide and Related Materials Conference (IPRM2005)*, Glasgow, Scotland, May 8-May 12 2005.

[9] C.T. Kirk, "A theory of Transistor Cut-off Frequency Fall-off at High Current Densities," *IRE Transactions on Electron Devices*, pp. 164-174, March 1962.

[10] W. Liu, Fundamentals of III-V Devices; HBTs, MESFETs, and HFETs/HEMTs, John Wiley & Sons, Inc., pp. 186-196, 1999.

[11] P. Velling, Zur metallorganischen Gasphasenepitaxie (MOVPE) mittels nicht-gasförmiger Quellen für elektronische Heterostruktur-Bauelemente basirend auf III/V-Halbleitern, PhD Thesis, Gerhard-Mercator-Universität Duisburg, 2002.

[12] M. Ida, et al., "Ultrahigh-Speed InP/InGaAs DHBTs with very High Current Density," *IEICE Trans. Electron.*, Vol. E86, No.10, pp. 1923-1928, October 2003.

[13] S. Topaloglu, "InP/InGaAs etching with Cl2/N2 ICP-RIE for HBT applications", *Oxford Plasma Technology, III/V Workshop on dry etching, plasma deposition, sputtering, MBE, Ion Beam processing*, OPT and FIRST Lab, ETH Zurich, Switzerland, 13-14 September 2005.

[14] P. Zampardi, et. al, "Delay of Kirk Effect Due to Collector Current Spreading in Heterojunction Bipolar Transistors", *IEEE Electron Device Letters*, Vol. 17, No. 10, October 1996.